American Industrial Hygiene Association Journal
Publication details, including instructions for authors and subscription information:
http://www.tandfonline.com/loi/aiha20

The Particle Size Distribution, Density, and Specific Surface Area of Welding Fumes from Smaw and GMAW Mild and Stainless Steel Consumables

Paul Hewett [a]

[a] National Institute for Occupational Safety and Health, 1095 Willowdale Road, Morgantown, WV 26505-2845

Published online: 04 Jun 2010.

To cite this article: Paul Hewett (1995) The Particle Size Distribution, Density, and Specific Surface Area of Welding Fumes from Smaw and GMAW Mild and Stainless Steel Consumables, American Industrial Hygiene Association Journal, 56:2, 128-135

To link to this article: http://dx.doi.org/10.1080/15428119591017150

AIHA JOURNAL Advances in Industrial & Environmental Hygiene

AM. IND. HYG. ASSOC. J. 56:128–135 (1995)

THE PARTICLE SIZE DISTRIBUTION, DENSITY, AND SPECIFIC SURFACE AREA OF WELDING FUMES FROM SMAW AND GMAW MILD AND STAINLESS STEEL CONSUMABLES

Paul Hewett

National Institute for Occupational Safety and Health, 1095 Willowdale Road, Morgantown, WV 26505-2845

Particle size distributions were measured for fumes from mild steel (MS) and stainless steel (SS); shielded metal arc welding (SMAW) and gas metal arc welding (GMAW) consumables. Up to six samples of each type of fume were collected in a test chamber using a micro-orifice uniform deposit (cascade) impactor. Bulk samples were collected for bulk fume density and specific surface area analysis. Additional impactor samples were collected using polycarbonate substrates and analyzed for elemental content. The parameters of the underlying mass distributions were estimated using a nonlinear least squares analysis method that fits a smooth curve to the mass fraction distribution histograms of all samples for each type of fume. The mass distributions for all four consumables were unimodal and well described by a lognormal distribution; with the exception of the GMAW-MS and GMAW-SS comparison, they were statistically different. The estimated mass distribution geometric means for the SMAW-MS and SMAW-SS consumables were 0.59 and 0.46 μm aerodynamic equivalent diameter (AED), respectively, and 0.25 μm AED for both the GMAW-MS and GMAW-SS consumables. The bulk fume densities and specific surface areas were similar for the SMAW-MS and SMAW-SS consumables and for the GMAW-MS and GMAW-SS consumables, but differed between SMAW and GMAW. The distribution of metals was similar to the mass distributions. Particle size distributions and physical properties of the fumes were considerably different when categorized by welding method. Within each welding method there was little difference between MS and SS fumes.

This article summarizes the results of a laboratory-based study of welding fumes.[1] One goal of the study was to measure the fume density, fume specific surface area, particle size distribution (PSD), and distribution of metals for each of four welding fumes. The results of these measurements are reported here. Another goal was to use these data to estimate both regional lung deposition and exposure (for example, inhalable particulate mass) for each type of fume. These estimates are reported and discussed in a companion paper.[2]

Mention of company or product names does not constitute an endorsement by the National Institute for Occupational Safety and Health.

BACKGROUND

The epidemiologic literature regarding welder's health is unclear on issues of chronic lung disease or lung cancer. In 1988 the National Institute for Occupational Safety and Health (NIOSH) reviewed the literature and concluded that welding is associated with metal fume fever, pneumonitis, chronic bronchitis, pneumonia, and decrements in pulmonary function, as well as a 40% excess of respiratory cancer.[3] While recognizing that the excess lung cancers may be related to exposures to stainless steel welding fumes, NIOSH recommended that all welding exposure concentrations, regardless of source, be reduced to the lowest feasible level using existing exposure limits as the "upper boundaries of exposure." In contrast, Morgan[4] reviewed the literature on both morbidity and mortality and concluded that the "evidence suggests that welding is not a particularly hazardous occupation provided care is taken to limit exposure to . . . any fumes that are generated." A recent mortality study involving 4459 welders of mild steel found that the standardized mortality ratio (SMR) for lung cancer was only 7% greater than expected (versus 17% greater than expected in the control group).[5] Another recent mortality study involving 11 092 welders with both mild steel and stainless steel welding experience observed a 34% increase in lung cancers.[6] A cross-sectional study of 135 shipyard welders[7] with an average of 33 years of exposure concluded that welding may be related to obstructive lung disease, but did not result in any "dramatic overt ill-health;" whereas, a longitudinal study of 609 shipyard welders[8] concluded that welding fumes interacted with smoking and atopic constitution to cause respiratory impairment. A cross-sectional study of 226 construction welders concluded that welding fumes and gases

TABLE I. Welding Consumables and Processes Studied

Metal	*Consumable*	*Welding Process*
Mild steel (MS)	AWS[A] E7018 (fluoride flux) 0.3175 cm ($\frac{1}{8}$ inch) electrode	SMAW[B]
	AWS E70S-3 0.0889 cm (0.035 inch) copper coated welding wire	GMAW[C]
Stainless steel (SS)	AWS E308-16 (fluoride flux) 0.3175 cm ($\frac{1}{8}$ inch) electrode	SMAW
	AWS ER308 0.0889 cm (0.035 inch) welding wire	GMAW

[A] American Welding Society
[B] Shielded metal-arc welding
[C] Gas metal-arc welding

cause chronic airway obstruction, but to a lesser extent than does smoking.[9]

This is only a sample of the published studies and reviews regarding the health of welders. Regardless of how the results of past studies are interpreted, Morgan's[4] admonition that "the technical aspects are constantly undergoing change, and continued vigilance is necessary lest a new process introduce a formerly unrecognized hazard" is still valid. Along these same lines Stern[10] suggested that the risk of disease in welders may depend on the welding process and/or welding consumable.

GMAW is a newer process that is increasing in popularity. Future studies of welders may include both SMAW and GMAW welders in the study cohort. Before doing exposure-response studies, the particle size distribution should be measured for each exposure group within the cohort.[11] This is because the PSD affects the relationship between the response variable, such as excess decrement in FEV_1, and exposure: there will be a different exposure-response relationship for each different PSD. If the distributions are similar, then a measure of exposure, such as "total (inhalable) welding fume," can be used as a surrogate measure of actual deposited particulate. If the distributions are substantially different, then estimates of deposited particulate are more appropriate and should, in principle, increase the probability of observing an exposure-response relationship. This article presents the results of a study of the particle size distributions and physical characteristics (fume density and specific surface area) of fumes from both SMAW and GMAW.

METHODS

The most common types of welding processes and welding metals were selected for this study: shielded metal arc welding (SMAW) and gas metal arc welding (GMAW), mild steel (MS) and stainless steel (SS). SMAW refers to the use of a flux-coated welding rod as the consumable electrode. During the welding process the rod melts and fuses with the base metal. The molten flux covers the molten metal to prevent oxidation during cooling.[12] GMAW welding refers to the use of machine-fed wire as the consumable electrode. Stainless steel wire is uncoated, while mild steel wire is coated with a thin layer of copper. An inert shield gas, argon in this study, provides protection from the atmosphere until the molten metal hardens. The consumables selected are listed in Table I. These consumables are commonly encountered in welding operations.

Welding Fume Generation and Sampling System

Welding fumes were generated inside a steel chamber (Figure 1). Base metals for welding consisted of either clean mild steel or stainless steel squares (30 × 30 cm and 0.64 cm [0.25 inch] thick), depending on the type of welding consumable. A Miller Dialarc® HF Constant Current AC/DC Arc Welding Power Source welding machine (Miller Electric Manufacturing Company, Appleton, Wis.) was used for both rod and wire welding. A straight bead was run the width of the square, with successive beads slightly overlapping to simulate actual welding, where a weld joint is built by laying successive layers of weld metal. The movable local exhaust hood of a United Air Specialists, Inc. (Cincinnati, Ohio) Smog Hog was placed over the opening at the top of the chamber, drawing all fumes upward. The inlet to the sampling system was placed in the opening (Figure 1). Fumes not captured by the sampling system inlet were captured by the local exhaust hood and removed by high efficiency filters.

The sampling system (Figure 1) consisted of a sharp-edged inlet, transport tubing, a single 90° bend, a sampling plenum, and sampling ports in the plenum for several filter cassettes used to collect a bulk fume sample and for a cascade impactor capable of resolving the particle size distributions of submicrometer aerosols. Stainless steel construction was used throughout.

The sampling system was designed to (1) draw a sample of the original aerosol into the sampling system inlet, (2) minimize particle losses within the transportation line and plenum, and (3) ensure as much as possible that each collection device sampled an identical PSD. The first two criteria were met by sampling

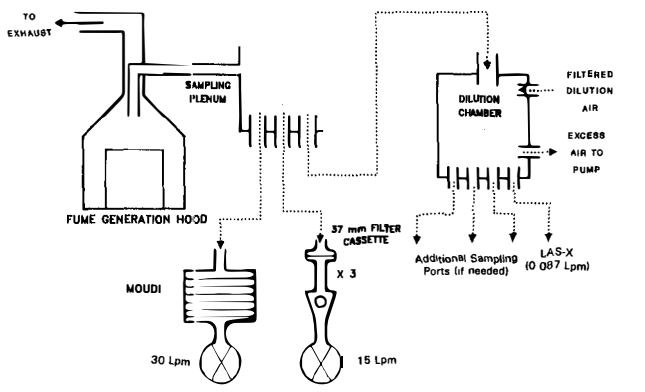

FIGURE 1. Schematic of fume generation hood, sampling plenum, and sampling equipment

near isokinetically at the inlet and minimizing the length of transport tubing and the number of 90° bends. The third criteria was met by using a single sampling probe and transport line to provide welding fume to all collection devices. The transport line fed into a small plenum to which all sampling devices were connected. Because particle losses within the sampling system may bias the observed PSD toward the smaller particle sizes, published formulae were used to estimate aspiration bias, losses just inside the inlet, line losses due to sedimentation and diffusion, and elbow losses due to inertial impaction. These estimates were combined into an estimated system collection efficiency as a function of particle size (see Reference 1 for details). The estimated system collection efficiency exceeded 95% for all particles less than 5 μm AED and 80% for particles between 5 and 10 μm AED.

Micro-Orifice Uniform Deposit Impactor (MOUDI)

The MOUDI (MSP Corporation, Minneapolis, Minn.) aerosol sampler is basically a conventional cascade impactor, but with two very important improvements. First, during sampling the impaction surfaces are constantly rotated beneath the stage orifices resulting in a nearly uniform circular deposition pattern. This reduces overloading and subsequent blowoff, which tends to skew the observed distributions toward the smaller sizes. Second, the lower stages have as many as 2000 small orifices (called micro-orifices) with diameters as small as 50 μm. The advantage to this is that the stage cutpoints can go as low as 0.05 μm aerodynamic diameter, with a pressure drop of one half atmosphere.[13-15] The MOUDI operates at 30 L/min (free airflow rate at the inlet). The pressure drop across the entire impactor is approximately 25 cm Hg, thus requiring a heavy-duty carbon vane vacuum pump. The actual stage cutpoints vary from impactor to impactor. The MOUDI used here had nine stages with cutpoints ranging from 0.071 to 15 μm aerodynamic diameter (Table II). The resulting mass distribution is in terms of the particle aerodynamic diameters.

Precut 46-mm diameter aluminum foil discs were used as impaction surfaces. Each foil was coated with a thin layer of silicone grease applied to the central portion of the substrate where impaction occurs. The final filter was a 37-mm diameter 2 μm pore size Gelman Teflon® filter (Gelman Sciences, Inc., Ann Arbor, Mich.). The impaction foils and final filters were pre-and post-weighed to within ± 0.02 mg using a Cahn C-31 microbalance (Cahn Instruments, Inc., Cerritos, Calif.) located in a climate controlled chamber.

Bulk Density and Specific Surface Area Determination

Bulk samples were collected using 37-mm diameter 0.8-μm pore size Gelman DM-800 filters (Gelman Sciences, Ann Arbor, Mich.). Six filters were loaded with particulate by sampling at high flow rates (greater than 20 L/min) while welding for approximately of 30 minutes. The caked particulate was scraped from each filter into a plastic vial and submitted to Micromeritics (Norcross, Ga.) for bulk density and specific surface area analysis. The fume bulk density was measured by micropycnometry using an Micromeritics AccuPyc 1330. Fume specific surface area was measured by the gas adsorption method using a Micromeritics Digisorb 2600 . The sample quantities submitted ranged from 70 to 100 mg.

TABLE II. Number and Size of Stage Orifices for the "Micro Orifice Uniform Deposit [Cascade] Impactor" Used in this Study

Stage	Number of Orifices	Orifice Size (cm)	Cutpoint d_{50} (μm)
0	1	1.7	15
1	10	0.38	5.6
2	10	0.247	3.2
3	20	0.137	1.8
4	40	0.072	1.0
5	80	0.040	0.57
6	900	0.014	0.31
7	900	0.009	0.155
8	2000	0.0055	0.071
Filter	—	—	<0.071

Elemental PSDs

Elemental PSDs were estimated by analyzing the MOUDI impactor substrates with inductively coupled plasma-atomic emission spectroscopy (NIOSH Method 7300).[16] For this analysis the conventional foil substrates were replaced with substrates made from polycarbonate Nucleopore filter material (Nucleopore, Pleasanton, Calif.). The impaction region in the center of each substrate was coated with silicone grease to prevent particle bounce and reentrainment. The final filter was a 37-mm diameter 2 μm pore size Zefluor Teflon filter (Gelman Sciences, Inc., Ann Arbor, Mich.). A single set of impactor substrates for each type of fume were submitted to the NIOSH Measurement Research Support Branch, Cincinnati, Ohio, for metals analysis. Each polycarbonyate substrate was wet ashed with a solution of concentrated nitric and perchloric acid. The final filters were wet ashed overnight to ensure that all particles embedded in the filter went into solution. Following the ashing procedure each sample was analyzed for iron, manganese, nickel, and chromium using inductively coupled plasma atomic emission spectroscopy. The results were plotted as histograms to determine if there were any substantial differences between the mass distributions and the elemental distributions.

DATA ANALYSIS METHODS

There were three categories of data analysis. The first involved the relatively simple calculation of mass fraction distribution histograms from the MOUDI data for each consumable. The second involved statistical comparisons to determine if the mass distributions were significantly different. For example, the six cascade impactor samples of the SMAW-MS fumes were compared to six samples of the SMAW-SS fume. The third category involved estimating the parameters of the underlying mass distribution for

TABLE III. Specific Surface Area (SSA) and Bulk Density Results[A]

Consumable[B]	SSA, m^2/g (sd)	Bulk Density, g/cm^3 (sd)
SMAW-MS	18.0 (0.1)	3.4 (0.1)
SMAW-SS	19.4 (0.2)	3.4 (0.1)
GMAW-MS	27.2 (0.2)	5.7 (0.2)
GMAW-SS	39.6 (0.3)	5.9 (0.6)

[A] Analysis by Micromeritics, Norcross, Georgia. Values in parentheses represent the standard deviation of the measurement, not the standard deviation of replicate samples.
[B] SMAW-MS = shielded metal arc welding—mild steel
SMAW-SS = shielded metal arc welding—stainless steel
GMAW-MS = gas metal arc welding—mild steel
GMAW-SS = gas metal arc welding—stainless steel

each consumable using a nonlinear least squares technique. Only an outline of the various calculations is presented here. With the exception of the statistical comparisons, all calculations were done using personal computer spreadsheet programs. Details are available in Reference 1.

Calculation of Mass Distribution Histograms

Average mass probability density distributions (hereafter referred to as mass distributions) were calculated by dividing the mass per stage per sample by the total mass collected per sample, and averaging across all samples. The average mass per stage was then divided by the aerodynamic diameter interval width (expressed in $\log_{10}$ units). This resulted in mass per log(d), which is graphed as a mass distribution histogram.

Comparison of PSDs

It was necessary to compare the size distribution data from one welding consumable to another. This was basically a comparison of two arrays, where each array consisted of five or six sets of mass per stage data. A test related to the t-test, Hotelling's T^2 two-sample test,[17] was used to make this comparison. The T^2 test allows multiple group comparison t-tests, while controlling the overall Type-I error. It was designed for situations where the data are not independent but related in some fashion. This method is appropriate for comparing cascade impactor data, because the mass fractions on each stage are related: each fraction was collected from the same mass distribution and depends on the penetration characteristics of the previous stages. A personal computer statistics package (SYSTAT Version 6.0, SYSTAT, Inc., Evanston, Ill.) was used to make these calculations. The null hypothesis was H_o: taken as a whole, $\mu_{11} = \mu_{22}$, . . . , $\mu_{1i} = \mu_{2i}$, . . . , $\mu_{1m} = \mu_{2m}$; where μ is the mean fraction for the i^{th} stage and the subscripts 1 and 2 refer to two different consumables. The test statistic is an F-value with m and $n_1 + n_2 - m - 1$ degrees of freedom, where n_1 and n_2 are the number

TABLE V. Comparison of the MOUDI Mass Fractions Using Hotelling's T^2 Two-Sample Test[A]

Consumable[B]	SMAW-SS (n = 6)	GMAW-MS (n = 6)	GMAW-SS (n = 5)
SMAW-MS (n = 6)	0.003[C]	<0.001[D]	<0.001[D]
SMAW-SS (n = 6)		0.001[D]	<0.001[D]
GMAW-MS (n = 6)			0.096[E]

[A] H_o: taken as a whole, the mean stage fractions were the same across those stages containing more than 5% of the total mass. Values are probabilities that the observed or greater differences would occur if H_o were true.
[B] SMAW-MS = shielded metal arc welding—mild steel
SMAW-SS = shielded metal arc welding—stainless steel
GMAW-MS = gas metal arc welding—mild steel
GMAW-SS = gas metal arc welding—stainless steel
[C] Comparison of stages 4, 5, 6, and 7
[D] Comparison of stages 4, 5, 6, 7, 8, and the final filter
[E] Comparison of stages 6, 7, 8, and the final filter

TABLE IV. PSD Data for Two Welding Rods and Two Welding Wires Expressed As Average Mass Fraction per Stage of the MOUDI[A]

Cutpoint (μm)	Stage	SMAW-MS[B] (AWS E7018) (n = 6) $\bar{x}$	s	SMAW-SS[B] (AWS E308-16) (n = 6) $\bar{x}$	s	MAW-MS[B] (AWS E70S-3) (n = 6) $\bar{x}$	s	GMAW-SS[B] (AWS ER308) (n = 5) $\bar{x}$	s
15	0	0.005	0.004	0.010	0.005	0.014	0.011	0.024	0.015
5.6	1	0.011	0.003	0.014	0.008	0.024	0.015	0.037	0.020
3.2	2	0.009	0.005	0.009	0.006	0.013	0.009	0.019	0.019
1.8	3	0.023	0.008	0.011	0.007	0.007	0.007	0.021	0.015
1.0	4	0.141	0.041	0.045	0.023	0.016	0.011	0.019	0.007
0.57	5	0.304	0.081	0.191	0.085	0.029	0.009	0.022	0.009
0.31	6	0.359	0.060	0.521	0.047	0.299	0.065	0.197	0.028
0.155	7	0.121	0.016	0.172	0.024	0.445	0.032	0.452	0.023
0.071	8	0.015	0.007	0.014	0.006	0.100	0.036	0.127	0.012
<0.071	F	0.011	0.002	0.014	0.006	0.053	0.014	0.083	0.020

[A] Due to rounding the mass fractions may not sum to one.
[B] SMAW-MS = shielded metal arc welding—mild steel
SMAW-SS = shielded metal arc welding—stainless steel
GMAW-MS = gas metal arc welding—mild steel
GMAW-SS = gas metal arc welding—stainless steel

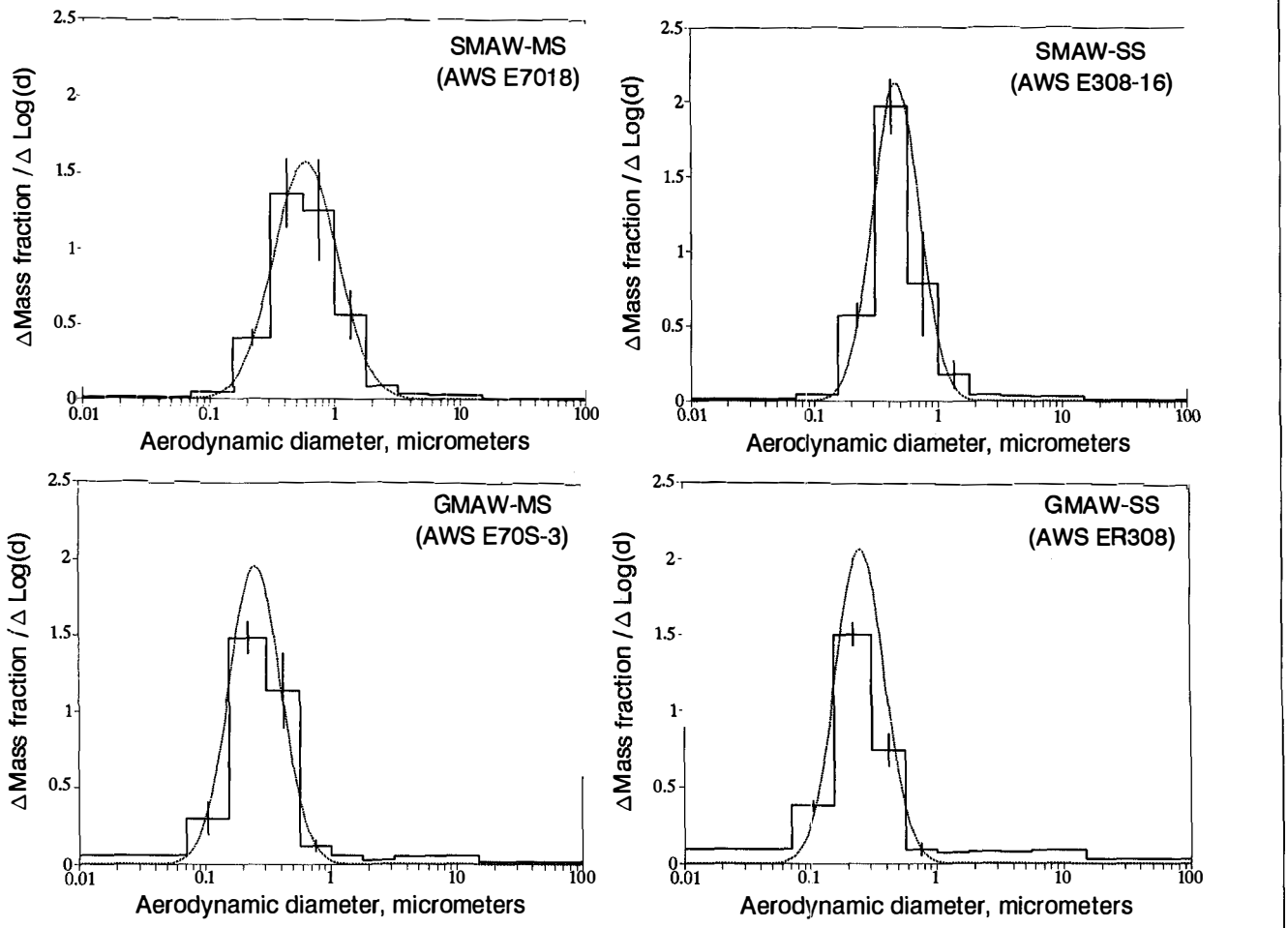

FIGURE 2. Graphs of the average mass distribution histograms and mass distribution curves estimated using nonlinear least squares analysis. Error bars indicate ± 1 standard deviation for the data.

of samples for the two consumables, and m is the number of variables. The alternative hypothesis was H_a: taken as a whole, the means are not equal. The MOUDI data contained 10 variables: weights from 9 stages and the final filter. Since the minimum degrees of freedom is one, the minimum comparison F-value was F^1_{10}. The minimum number of samples, per consumable, for a comparison across all stages was six (since $n_1 + n_2 - 10 - 1 \geq 1$, $n_1 + n_2 \geq 12$).

Estimation of the Underlying Distribution Parameters

The mass fraction collected at each stage of an impactor depends not only on the mass distribution and the impactor stage cutpoint, but also on the stage penetration characteristics. An iterative analysis technique known as the method of nonlinear least squares was used to fit a smooth curve to the observed histograms and estimate the parameters of the underlying distribution, while taking into account the nonideal stage penetration characteristics. The nonlinear least squares method is used in those cases where a function f(x) is neither linear in its parameters, nor is there a transformation that results in linear parameters.[18] In this case the author wanted to describe the mass fraction collected on each impactor stage as a function of PSD, be it unimodal or multimodal; impactor stage cutoff diameter; and the stage penetration efficiency characteristics. This procedure is a modification of a curve-fitting technique developed earlier.[19] There are six steps to this procedure:

(1) Calculate and graph the (observed) mass frequency histogram using a personal computer spreadsheet program.
(2) By visual inspection of the histogram, estimate the parameters of the true distribution from which the observed histogram was derived: the number of modes or underlying distributions, the GM and GSD of each mode or underlying distribution, and the percentage each mode comprises of the overall distribution.
(3) Calculate and graph the mass fraction distribution function for this set of parameters.
(4) Using the impactor collection efficiency curves, calculate the histogram expected to result if this distribution were sampled.
(5) Simultaneously display the observed histogram from step (1) and the simulated histogram from step (4) and calculate the fit factor (a measure of the goodness-of-fit, discussed later).

TABLE VI. Mass Median Aerodynamic Diameter (MMAD; Geometric Mean of the Mass Distribution) and Geometric Standard Deviation for Each Type of Fume

Consumable[A]	MMAD (μm)	GSD
SMAW-MS	0.59	1.80
SMAW-SS	0.46	1.55
GMAW-MS	0.24	1.65
GMAW-SS	0.25	1.55

[A] SMAW-MS = shielded metal arc welding—mild steel
SMAW-SS = shielded metal arc welding—stainless steel
GMAW-MS = gas metal arc welding—mild steel
GMAW-SS = gas metal arc welding—stainless steel

(6) Change the distribution parameters until a satisfactory fit is obtained, as indicated by an expected histogram that closely matches the observed histogram and a low fit factor.

The author wrote a spreadsheet "macro" program to automate Step 6, so that the result is an objective estimate of the parameters of the true mass distribution. The basis for this method is as follows. It is reasonable to describe multimodal or combined PSDs by a linear combination of weighted lognormal distributions:

$$f_c(x) = a_1 f_1(x) + a_2 f_2(x) + \cdots + a_n f_n(x) \quad (1)$$

where x is the particle aerodynamic diameter; $f_c(x)$ is the combined mass distribution (probability density) function; $f_n(x)$ is the mass distribution function for the n^{th} underlying distribution; and a_n represents the distribution coefficient, or fraction of the overall distribution, for the n^{th} underlying distribution.

The mass distribution function for each distribution, at any x, can be calculated:

$$f_n(x) = \frac{1}{\log_{10} GSD_n \sqrt{2\pi}} \exp\left(\frac{-(\ln x - \ln GM_n)^2}{2(\ln GSD_n)^2}\right) \quad (2)$$

where GM_n and GSD_n are the geometric mean and geometric standard deviation of the n^{th} underlying distribution. Equation 2 yields frequency values for the $\log_{10}$ scale.

Cascade impactor collection efficiency curves are s-shaped, according to both theory and observation. The functional form of the curves can be approximated using a two-parameter cumulative lognormal function.[20] Penetration efficiency for any diameter can be calculated by the complement of the cumulative function:

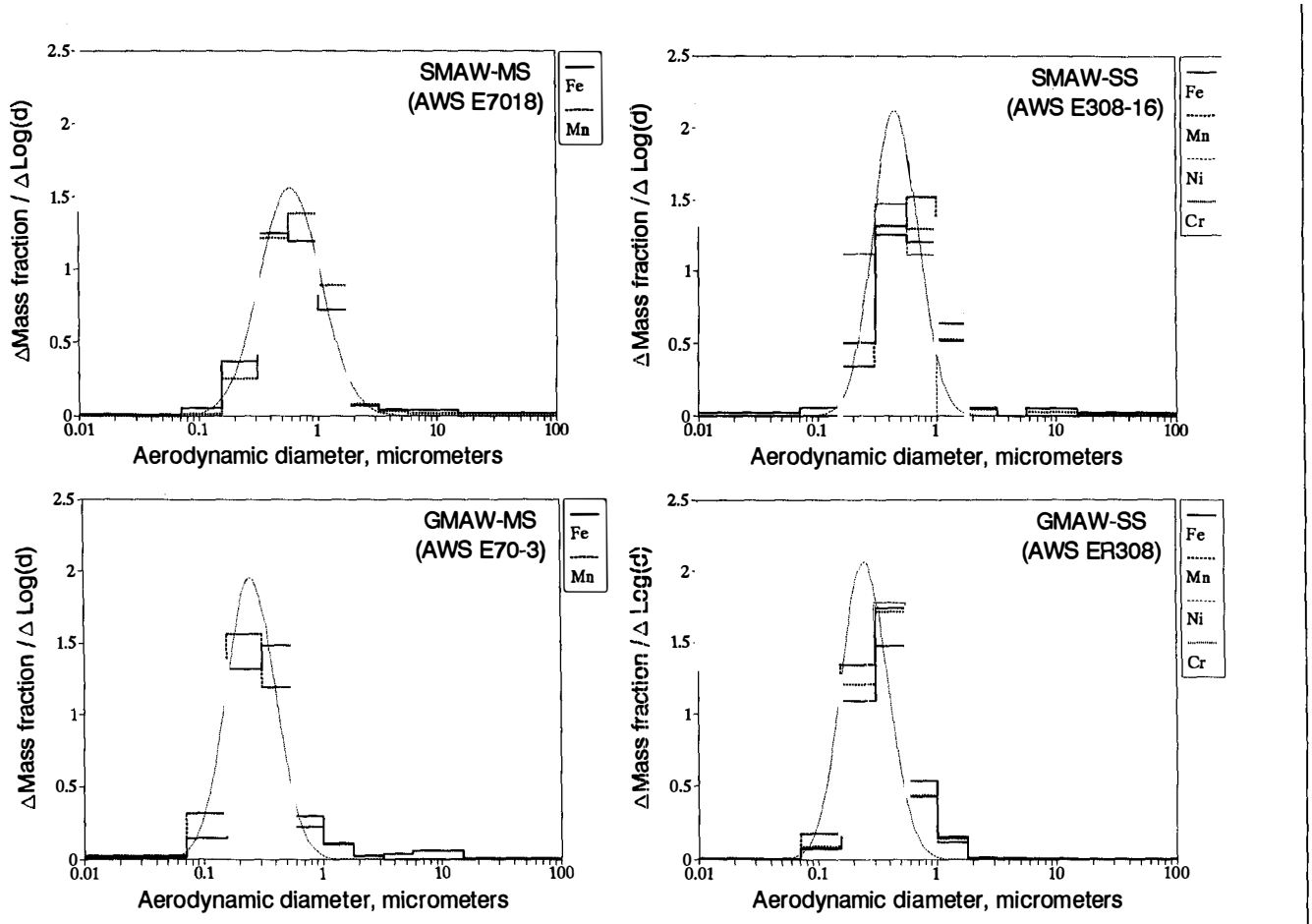

FIGURE 3. Elemental mass distribution histograms for each welding rod and wire

$$P(x) = 1 - \int_{x_1}^{x} \frac{1}{\log_{10} GSD\sqrt{2\pi}} \exp\left(\frac{-(\ln x - \ln GM)^2}{2(\ln GSD)^2}\right)dx \quad (3)$$

where x_1 is an arbitrary lower limit. The GM is the impactor stage cutpoint (d_{50}) and the GSD is set at a value that allows the resulting curve to closely fit the impactor stage calibration data. Marple et al.[15] found that the penetration efficiency curves for Stages 1 through 5 of the MOUDI impactor had a GSD of 1.08. The datapoints in Figure 5 of Reference 15 were used to assign GSDs of 1.4, 1.2, 1.2, and 1.3 to the penetration curves of Stages 0, 6, 7, and 8. (The GSDs were estimated using log-probit regression.)

Given a distribution described by Equation 1, the fraction (e_i) of the overall distribution expected to deposit on the i^{th} impactor stage is given by:

$$e_i = \int_{x_1}^{x_2} f_c(x)[1 - P_i(x)]\left[\prod_{j=1}^{i-1} P_j(x)\right]dx \quad (4)$$

where x_1 is an arbitrary lower boundary of the distribution, x_2 is an arbitrary upper boundary, and $P_i(x)$ is the penetration efficiency function (Equation 3) of the i^{th} impactor stage.

Using Bevington[18] as a guide, the author defined a fit factor:

$$\text{fit factor} = \frac{1}{nm - p}\sum_{i=1}^{m}\sum_{j=1}^{n}\frac{1}{\sigma_i^2}(o_{ij} - e_i)^2 \quad (5)$$

where o_{ij} and e_i are the observed and expected mass fractions, respectively, for the i^{th} stage and j^{th} sample; n is the number of samples; m is the number of stages; and p is the number of parameters estimated from the data. One requirement is that the number of stages must exceed the number of parameters: $m - p \geq 1$. The variance (σ_i^2) was estimated by the sample variance (s_i^2). The fit factor is similar to the "reduced χ^2" (reduced chi square) described by Bevington.[18]

RESULTS AND DISCUSSION

During the actual welding every effort was made to maintain a constant arc length that was consistent with producing a smooth weld, as the arc length has been shown to affect the quantity of fume produced[21] and probably the PSD as well.

Bulk Density and Specific Surface Area Analysis

The bulk densities for the fumes generated using SMAW-MS and SMAW-SS welding rods were, after rounding, identical at 3.4 g/cm^3, despite the differences in rod compositions (Table III). The bulk densities for the fumes generated using GMAW-MS and GMAW-SS welding wires were 5.7 and 5.9 g/cm^3, respectively. These bulk densities are consistent with the elemental composition of the fumes. The fumes from the SMAW rods, such as the SMAW-MS and SMAW-SS welding rods, contain large percentages of low density elements, such as calcium, potassium, and fluorine.[22] Fumes from GMAW wires, such as the GMAW-MS wire, consist almost entirely of metal oxides.

The specific surface area estimates for the SMAW-MS and SMAW-SS fumes were similar at 18.0 and 19.4 m^2/g, respectively. The specific surface area estimates for the GMAW-MS and GMAW-SS fumes were 27.2 and 39.6 m^2/g, respectively.

These results are similar to those reported by Hewitt and Gray.[23] They reported a specific surface area and bulk density of 13 m^2/g and 3 g/cm^3, respectively, for SMAW fumes, and a specific surface area of 30 m^2/g for GMAW fumes.

Comparison of Welding Fumes Using the Impactor Stage Mass Fractions

Six MOUDI impactor samples were collected for each of the SMAW-MS, E308-16, and E70S-3 consumables and five samples for the GMAW-SS wire. Table IV contains the average mass fractions per stage for the four SMAW and GMAW consumables. The average mass fractions may not sum to one due to rounding.

Hotelling's T^2 two-sample test was used to determine if the impactor stage loadings were statistically different among the four consumables. When comparing across all stages, none of the T^2 statistics were statistically significant at the $p < 0.05$ significance level, with the exception of the SMAW-SS versus GMAW-SS comparison. However, the p-values were low, which suggested that some differences do exist that were obscured, perhaps by the highly variable data (relative to the means) on the lighter loaded impactor stages. When the test was restricted to those stages containing, on average, more than 5% of the mass, all of the comparisons were statistically significant at the $p < 0.05$ significance level with the exception of the GMAW-MS versus GMAW-SS comparison, which was significant at the $p < 0.1$ significance level (Table V).

Estimation of the Underlying Mass Distribution Parameters

Since the average histogram for each consumable did not appear to be obviously bimodal, a unimodal curve, described by a single GM and GSD, was fit to the histograms for each type of fume using the nonlinear least squares analysis technique. The fit-factor (Equation 5) took into account the variability in the observed data allowing a unimodal smooth curve to be fit to all samples simultaneously. The average mass distribution histograms and the fitted smooth curves are graphed in Figure 2. The estimated mass distribution geometric means, expressed as aerodynamic diameters, and geometric standard deviations are given in Table VI.

The American Welding Society[24] reported distributions derived from cascade impactor data where 100% of the SMAW fumes were less than 1 μm AED, and nearly 100% of the GMAW fumes were below 0.5 μm AED. The parameters of the mass distributions were not presented due to the fact that nearly 100% of the mass was deposited on the backup filter and the last stage of the impactor. The distribution parameters reported here are consistent with these earlier findings.

Elemental PSDs

The element distribution histograms (Figure 3) appear similar to the average mass histograms (Figure 2) indicating that the metals were evenly distributed throughout each PSD. Therefore, deposition of a particular metal should not differ significantly from that of the overall aerosol. No statistical tests were utilized due to the lack of replicate samples.

CONCLUSIONS

(1) The bulk fume densities and specific surface areas were greater for the welding wires than for the welding rods. The differences were primarily related to process (SMAW versus GMAW) and not consumable type (mild steel versus stainless steel).

(2) The mass PSDs, determined by inertial impaction, for the two welding rods (SMAW-MS and SMAW-SS) and the two welding wires (GMAW-MS and GMAW-SS) were similar in shape, and all basically consisted of submicrometer particles. The mass distributions for the welding wires were shifted to the smaller particle sizes compared to those for the welding rods.

(3) The MOUDI elemental mass frequency histograms (Figure 3) appeared similar to the average mass histograms (Figure 2), suggesting that the metals were evenly distributed across the PSDs. Therefore, predictions of deposition and exposure for the overall aerosol also should apply to the individual metals.

ACKNOWLEDGMENTS

This article summarizes a portion of the work done for a doctoral degree in industrial hygiene at the School of Public Health, University of Pittsburgh. The author wishes to thank NIOSH for supporting him in the pursuit of this degree; Dr. Nurtan A. Esmen for serving as his advisor through both thick and thin; Dr. Sidney Soderholm for his many helpful suggestions regarding the draft manuscript; Mark Millson (NIOSH) for the elemental analysis; and Micromeritics for the density and specific surface area analysis.

REFERENCES

1. **Hewett, P.:** "Particle Size Analysis of Welding Fumes and Prediction of Pulmonary Deposition." Ph.D. diss., School of Public Health, University of Pittsburgh, Pittsburgh, PA. Available from *Dissertation Abstracts International* vol. 52-10B; University Microfilms, Ann Arbor, MI [Pub. #9209560], 1991.
2. **Hewett, P.:** Estimation of regional pulmonary deposition and exposure for welding fumes from SMAW and GMAW mild and stainless steel consumables. *Am. Ind. Hyg. Assoc. J. 56*:136–142 (1995).
3. **National Institute for Occupational Safety and Health (NIOSH):** *Criteria for a Recommended Standard—Welding, Brazing, and Thermal Cutting.* [DHHS (NIOSH) Pub. No. 88–110] Cincinnati, OH: NIOSH, 1988.
4. **Morgan, W.K.C.:** On welding, wheezing, and whimsy. *Am. Ind. Hyg. Assoc. J. 50*:59–69 (1989).
5. **Steenland, K., J. Beaumont, and L. Elliot:** Lung cancer in mild steel welders. *Am. J. Epidemiol. 133*:220–229 (1991).
6. **Simonato, L., A.C. Fletcher, A. Andersen, et al.:** A historical prospective study of European stainless steel, mild steel, and shipyard welders. *Br. J. Ind. Med. 48*:145–154 (1991).
7. **McMillan, G.H.G. and R.J. Pethybridge:** A clinical, radiological, and pulmonary function case-control study of 135 dockyard welders ages 45 years and over. *J. Soc. Occup. Med. 34*:3–23 (1984).
8. **Chinn, D.J., I.C. Stevenson, and J.E. Cotes:** Longitudinal respiratory survey of shipyard workers: effects of trade and atopic status. *Br. J. Ind. Med. 47*:83–90 (1990).
9. **Kilburn, K.H. and R.H. Warshaw:** Pulmonary functional impairment from years of arc welding. *Am. J. Med. 87*:62–69 (1989).
10. **Stern, R.M.:** Process-dependent risk of delayed health effects for welders. *Environ. Health Persp. 41*:235–253 (1981).
11. **Hewett, P.:** Limitations in the use of particle size selective sampling criteria in occupational epidemiology. *Appl. Occup Envion. Med. 6*:290–300 (1991).
12. **Griffiths, J.:** Minerals in welding fluxes—the whys and wherefores. *Ind. Minerals* March 1985, pp. 19–39.
13. **MSP Corporation:** *Instruction Manual—Model 100 Micro-Orifice Uniform Deposit Impactor (MOUDI®).* Minneapolis, MN: MSP Corp., 1989.
14. **Marple, V.A., K. Rubow, G. Ananth, and H.J. Fissan:** Micro-orifice uniform deposit impactor. *J. Aerosol Sci. 17*:489–494 (1986).
15. **Marple, V.A., K. Rubow, and S.M. Bahm:** A microorifice uniform deposit impactor (MOUDI): description, calibration, and use. *Aerosol Sci. and Technol. 14*:434–446 (1991).
16. **National Institute for Occupational Safety and Health (NIOSH):** *NIOSH Manual of Analytical Methods*, 3rd ed. Cincinnati, OH: NIOSH, 1984.
17. **Tatsuoka, M.M.:** *Multivariate Analysis: Techniques for Education and Psychological Research.* New York: John Wiley & Sons, 1971. p. 84.
18. **Bevington, P.R.:** *Data Reduction and Error Analysis for the Physical Sciences.* New York: McGraw-Hill, 1969.
19. **Hewett, P. and M.A. McCawley:** A microcomputer spreadsheet technique for analyzing multimodal particle size distributions. *Appl. Occup. Environ. Hyg. 6*:865–873 (1991).
20. **Rubow, K.L., V.A. Marple, J. Olin, and M.A. McCawley:** A personal cascade impactor: design, evaluation, and calibration. *Am. Ind. Hyg. Assoc. J. 48*:532–538 (1987).
21. **Heile, R.F. and D.C. Hill:** Particulate fume generation in arc welding processes. *Welding J. 54*:201s–201s (1975).
22. **Fasiska, E.J.:** *Characterization of Arc Welding Fume.* Miami: American Welding Society, 1983.
23. **Hewitt, P.J. and C.N. Gray:** Some difficulties in the assessment of electric arc welding fume. *Am. Ind. Hyg. Assoc. J. 44*:727–732 (1983).
24. **American Welding Society:** *The Welding Environment, a Research Report on Fumes and Gases Generated During Welding Operations.* Miami: American Welding Society, 1973.